Odd harmonics with wavelength modulation spectroscopy for recovering gas absorbance shape

Peng Zhimin,[1] Ding Yanjun,[1,*] Che Lu,[1] and Yang Qiansuo[2]

[1]*State Key Laboratory of Power Systems, Dept of Thermal Engineering, Tsinghua University, Beijing 100084, China*
[2]*Laboratory of High Temperature Gas Dynamics, Institute of Mechanics, CAS, Beijing, 100190, China*
[*]*dyj@tsinghua.edu.cn*

In this paper, a new method for recovering gas absorbance shape using wavelength modulation spectroscopy is proposed. We have mathematically proven that the gas absorbance shape can be directly recovered using the data of X and Y components of odd harmonics, regardless of the value of the modulation depth. The transitions of NH_3 near 1531 nm are selected to recover the absorbance shape using numerical simulation and experimental technique. The simulation and experiment results show that our proposed method can simply and accurately recover the gas absorbance shape.

©2012 Optical Society of America

OCIS codes: (300.1030) Absorption; (300.6260) Spectroscopy, diode lasers.

References and links

1. X. Liu, J. B. Jeffries, R. K. Hanson, K. M. Hinckley, and M. A. Woodmansee, "Development of a tunable diode laser sensor for measurements of gas turbine exhaust temperature," Appl. Phys. B **82**(3), 469–478 (2006).
2. R. Sur, T. J. Boucher, M. W. Renfro, and B. M. Cetegen, "In situ measurements of water vapor partial pressure and temperature dynamics in a PEM fuel cell," J. Electrochem. Soc. **157**(1), B45–B53 (2010).
3. H. Li, S. D. Wehe, and K. R. McManus, "Real-time equivalence ratio measurements in gas turbine combustors with a near-infrared diode laser sensor," Proc. Combust. Inst. **33**(1), 717–724 (2011).
4. N. Goldstein, S. Adler-Golden, J. Lee, and F. Bien, "Measurement of molecular concentrations and line parameters using line-locked second harmonic spectroscopy with an AlGaAs diode laser," Appl. Opt. **31**(18), 3409–3415 (1992).
5. A. Farooq, J. B. Jeffries, and R. K. Hanson, "CO₂ concentration and temperature sensor for combustion gases using diode-laser absorption near 2.7μm," Appl. Phys. B **90**(3–4), 619–628 (2008).
6. J. T. C. Liu, J. B. Jeffries, and R. K. Hanson, "Wavelength modulation absorption spectroscopy with *2f* detection using multiplexed diode lasers for rapid temperature measurements in gaseous flows," Appl. Phys. B **78**(3–4), 503–511 (2004).
7. E. D. Tommasi, G. Casa, and L. Gianfrani, "High precision determinations of NH₃ concentration by means of diode laser spectrometry at 2.005 μm," Appl. Phys. B **85**(2–3), 257–263 (2006).
8. G. B. Rieker, J. B. Jeffries, and R. K. Hanson, "Calibration-free wavelength-modulation spectroscopy for measurements of gas temperature and concentration in harsh environments," Appl. Opt. **48**(29), 5546–5560 (2009).
9. A. Farooq, J. B. Jeffries, and R. K. Hanson, "Sensitive detection of temperature behind reflected shock waves using wavelength modulation spectroscopy of CO₂ near 2.7μm," Appl. Phys. B **96**(1), 161–173 (2009).
10. K. Duffin, A. J. McGettrick, W. Johnstone, G. Stewart, and D. G. Moodie, "Tunable diode laser spectroscopy with wavelength modulation: A calibration-free approach to the recovery of absolute gas absorption line-shapes," J. Lightwave Technol. **25**(10), 3114–3125 (2007).
11. W. Johnstone, A. J. McGettrick, K. Duffin, A. Cheung, and G. Stewart, "Tunable diode laser spectroscopy for industrial process applications: System characterization in conventional and new approaches," IEEE Sens. J. **8**(7), 1079–1088 (2008).
12. A. J. McGettrick, K. Duffin, W. Johnstone, G. Stewart, and D. G. Moodie, "Tunable diode laser spectroscopy with wavelength modulation: A phasor decomposition method for calibrationfree measurements of gas concentration and pressure," J. Lightwave Technol. **26**(4), 432–440 (2008).
13. G. Stewart, W. Johnstone, J. R. P. Bain, K. Ruxton, and K. Duffin, "Recovery of absolute gas absorption line shapes using tunable diode laser spectroscopy with wavelength modulation—part 1: Theoretical analysis," J. Lightwave Technol. **29**(6), 811–821 (2011).

14. J. R. P. Bain, W. Johnstone, K. Ruxton, G. Stewart, M. Lengden, and K. Duffin, "Recovery of absolute gas absorption line shapes using tuneable diode laser spectroscopy with wavelength modulation—Part 2: Experimental investigation," J. Lightwave Technol. **29**(7), 987–996 (2011).
15. P. Kluczynski and O. Axner, "Theoretical description based on Fourier analysis of wavelength-modulation spectrometry in terms of analytical and background signals," Appl. Opt. **38**(27), 5803–5815 (1999).
16. P. Zhimin, D. Yanjun, C. Lu, L. Xiaohang, and Z. Kangjie, "Calibration-free wavelength modulated TDLAS under high absorbance conditions," Opt. Express **19**(23), 23104–23110 (2011).
17. A. N. Dharamsi, "A theory of modulation spectroscopy with applications of higher harmonic detection," J. Phys. D Appl. Phys. **29**(3), 540–549 (1996).
18. J. Henningsen and H. Simonsen, "Quantitative wavelength-modulation spectroscopy without certified gas mixtures," Appl. Phys. B **70**(4), 627–633 (2000).
19. H. Li, G. B. Rieker, X. Liu, J. B. Jeffries, and R. K. Hanson, "Extension of wavelength-modulation spectroscopy to large modulation depth for diode laser absorption measurements in high-pressure gases," Appl. Opt. **45**(5), 1052–1061 (2006).
20. H. Jia, W. X. Zhao, T. D. Cai, W. D. Chen, W. J. Zhang, and X. M. Gao, "Absorption spectroscopy of ammonia between 6526 and 6538cm^{-1}," J. Quant. Spectrosc. Radiat. Transf. **110**(6–7), 347–357 (2009).

1. Introduction

Recognizing the power of tunable diode laser absorption spectroscopy (TDLAS) for highly sensitive measurements, scientists have applied TDLAS in many areas to measure gas temperature, pressure, and concentration, and have achieved valuable research results in many areas [1–4]. During this period, direct absorption spectroscopy (DAS) has been used extensively for many years because of its simplicity, accuracy, and ability to directly determine gas temperature, concentration, pressure, and spectroscopic parameters according to the measured gas absorbance shape of the selected transitions [5]. However, with the development of the TDLAS and improvements in measurement, especially in very harsh industrial environments, DAS is easily influenced by particle concentration, laser intensity fluctuations, and baseline-fitting errors which often hamper the accurate determination of the gas absorbance shape. As a result, meeting measurement requirements becomes more and more difficult [6]. Wavelength modulation spectroscopy (WMS) is more sensitive by one or two orders of magnitude relative to the DAS, which can reduce or eliminate laser, $1/f$, and other types of noise in actual measurements [7]. However, WMS has some striking shortcomings that are difficult to address. For example, one of the key drawbacks in applying WMS for measuring gas concentration is the need to calibrate the WMS signals to a known mixture to recover the absolute concentration [8]. R. K. Hanson et al. recently developed a method to directly determine gas concentration by comparing experimental harmonic signals with theoretical values [9]. However, gas temperature, species concentration, total pressure, laser characteristics, absorption length, and spectroscopic parameters are essential requirements for calculating harmonic signals. Uncertainties in these parameters result in discrepancies between the numerical and experimental values, leading to gas concentration measurement errors.

Taking into account the shortcomings of WMS and the advantages of DAS (temperature, concentration, pressure and spectroscopic parameters determined by the gas absorbance shape), a team led by Professor G. Stewart [10–14] of Strathclyde University recently proposed a method to recover the gas absorbance shape using the first harmonic signal based on the residual amplitude modulation (RAM). G. Stewart's method, which uses the data of X and Y components of the first harmonic to recover the gas absorbance shape, and works well under small modulation indices ($m<0.2$) when the first harmonic profile is close to the true absorbance shape [10]. G. Stewart's method is very useful, especially in cases when DAS cannot measure the gas absorbance shape. However, G. Stewart's method only uses the first harmonic signal to recover the absorbance shape. Even higher-order terms (function of the modulation index), especially the second- and fourth-order terms will badly affect the recovery of results when greater modulation indices ($m>0.5$) are used. As their studies note, the recovering errors increase sharply as the modulation index increases in actual measurements [11]. In order to reduce or eliminate the effects of even higher-order terms and to expand the scope of

application of this technology, G. Stewart et al. attempted to calculate the effects of the even higher-order terms (until the fourth-order) using the Lorentzian shape to reduce the recovering errors in their earlier investigations, with the scope of application of the modulation index increased to 0.75 [12]. However, their computation process is quite complex, such that the effects of the even higher-order terms cannot be calculated when the absorbance shape is close to the Voigt profile. In recent studies, G. Stewart et al. introduced a "shape correction function" to correct the gas absorbance shape [13,14]. However, the problem is that the absorbance shape is the necessary condition to calculate such a function. Thus, the "shape correction function" can only be accurately calculated in laboratory conditions when absorbance shape is known. However, in actual measurements, the absorbance shape is an unknown parameter, and the "shape correction function" very difficult or impossible to calculate in many practical applications. Therefore, establishing an efficient and simple method to recover the gas absorbance shape is an urgent issue, particularly in the area of WMS.

To address the aforementioned problems, the present paper derives the X and Y component expressions of each harmonic based on the absorption and harmonic theories. On this basis, we have mathematically proven that the gas absorbance shape can be recovered directly, when the data of X and Y components of the odd harmonics are processed by our method. Finally, to validate the precision of our method, transitions of NH_3 near 1531 nm are selected to recover the gas absorbance shape using numerical simulation and experimental techniques.

2. Theory

The basic principle of WMS has been introduced in a number of studies [15–18]. Some of the basic theories presented here explain the derivation of the method established in this study. To produce harmonic signals, a sinusoidal modulation of the angular frequency ω rides on a slowly varying diode laser injection current, and the instantaneous laser frequency and intensity may be expressed as:

$$\begin{cases} v = v_1 + a\cos(\omega t), \\ I_0 = I_1 + \Delta I\cos(\omega t + \psi_1), \end{cases} \tag{1}$$

where a and ΔI are the amplitudes of modulation around v_1 and I_1, which are the slowly varying values of the laser frequency and intensity. Here, a is named as modulation depth in the following chapter, ψ_1 is the phase shift between the intensity and frequency modulation, which is strongly dependent on the modulation frequency. For the isolated transition, the modulation index can be defined as: $m = a/\gamma$, where γ is the half width at half-maximum (HWHM) of the transition.

The laser transmission of monochromatic radiation at frequency v through a uniform medium is given by the Beer–Lambert relation and can be expanded as follows:

$$\tau(v) = \frac{I_t}{I_0} = \exp\left[-\alpha(v)\right] = \frac{H_0}{2} + \sum_{k=1}^{\infty} H_k \cdot \cos(k\omega t), \tag{2}$$

where $\tau(v)$ is the laser transmission, I_t and I_0 are the laser transmitted and incident intensities, respectively, $\alpha(v)$ is the gas absorbance shape, and the functions H_k ($k = 0,1,2\ldots$) are given as follows:

$$H_k = \frac{1}{\pi}\int_{-\pi}^{\pi} \tau(v_1 + a\cos\theta)\cos k\theta \cdot d\theta. \tag{3}$$

Substituting I_0 into Eq. (2), the laser transmitted intensity can be written as:

$$I_t = C_{00} + \sum_{k=1}^{\infty} \left[C_{k1} \cdot \cos(k\omega t) + C_{k2} \cdot \sin(k\omega t) \right], \tag{4}$$

where C_{00}, C_{k1} and C_{k2} ($k = 1,2\ldots$) are given as:

$$\begin{cases} C_{00} = \dfrac{1}{2} \left(I_1 H_0 + \Delta I H_1 \cos \psi_1 \right), \\[2mm] C_{k1} = I_1 H_k + \dfrac{\Delta I}{2} \left(H_{k-1} + H_{k+1} \right) \cos \psi_1, \\[2mm] C_{k2} = \dfrac{\Delta I}{2} \left(-H_{k-1} + H_{k+1} \right) \sin \psi_1. \end{cases} \tag{5}$$

Based on the harmonic theory, lock-in measurements use a phase-sensitive detector to detect and measure very small signals, and the reference signals used to detect the X and Y components of the kth ($k = 1,2\ldots$) harmonic can be expressed as:

$$\begin{cases} R_{X-k} = V \cos(k\omega t + \beta), \\[1mm] R_{Y-k} = V \sin(k\omega t + \beta), \end{cases} \tag{6}$$

where V is the signal amplitude, and β is the phase shift between the reference and detection signals. Multiplying Eq. (4) and (6), the outputs of the X and Y components of the kth ($k = 1,2\ldots$) harmonic generated by the lock-in amplifier can be written as follows, where G is the electro optical gain of the detection system.

$$\begin{cases} X_k = \dfrac{GV}{2} \cdot \left[C_{k1} \cdot \cos(\beta) - C_{k2} \cdot \sin(\beta) \right], \\[2mm] Y_k = \dfrac{GV}{2} \cdot \left[C_{k1} \cdot \sin(\beta) + C_{k2} \cdot \cos(\beta) \right]. \end{cases} \tag{7}$$

In Eq. (3), when there is no absorption (laser transmission $\tau(v) = 1$), the $H_0 = 2$ and $H_k = 0$ ($k = 1,2\ldots$), the outputs of X and Y components of the first harmonic can be written as follows, where $S_{1\text{-}back}$ is the magnitude of the first harmonic when there is no gas absorption (defining as background signal).

$$\begin{cases} X_{1-back} = \dfrac{GV\Delta I}{2} \cos(\beta - \psi_1) \\[2mm] Y_{1-back} = \dfrac{GV\Delta I}{2} \sin(\beta - \psi_1) \end{cases} \Rightarrow S_{1-back} = \sqrt{\left(X_{1-back} \right)^2 + \left(Y_{1-back} \right)^2} = \dfrac{GV\Delta I}{2} \tag{8}$$

In Eq. (7), when the X and Y components of the odd harmonics are multiplied by $\sin\beta$ and $\cos\beta$, respectively, and are normalized by the background signal of the first harmonic, we can obtain the following equations:

$$fun_{2k-1} = \frac{X_{2k-1} \cdot \sin\beta - Y_{2k-1} \cdot \cos\beta}{S_{1-back}} = \frac{\sin\psi_1}{2} \cdot \left[H_{2k-2} - H_{2k} \right], \quad k = 1,2\ldots \tag{9}$$

In Eq. (3), according to Taylor's theory, the laser transmission $\tau(v_1 + a\cos\theta)$ can be expanded as a Taylor series around any particular frequency v_1 as follows:

$$\tau\left(v_1 + a\cos\theta\right) = \tau\left(v_1\right) + \sum_{k=1}^{\infty} \frac{\tau^{(k)}\left(v_1\right)\left(a\cos\theta\right)^k}{k!}. \tag{10}$$

Substituting Eq. (10) into Eq. (3), we can obtain:

$$\begin{cases} \dfrac{H_0}{2} = \tau\left(v_1\right) + \dfrac{\tau^{(2)}\left(v_1\right)a^2}{4} + \dfrac{\tau^{(4)}\left(v_1\right)a^4}{64} + \dfrac{\tau^{(6)}\left(v_1\right)a^6}{2304} + \ldots \\[2mm] H_2 = \dfrac{\tau^{(2)}\left(v_1\right)a^2}{4} + \dfrac{\tau^{(4)}\left(v_1\right)a^4}{48} + \dfrac{\tau^{(6)}\left(v_1\right)a^6}{1536} + \ldots \\[2mm] H_4 = \dfrac{\tau^{(4)}\left(v_1\right)a^4}{192} + \dfrac{\tau^{(6)}\left(v_1\right)a^6}{3840} + \ldots \\[2mm] H_{2k} = \displaystyle\sum_{n=k}^{\infty} \dfrac{1}{(n+k)!} \cdot \dfrac{1}{(n-k)!} \cdot \dfrac{1}{2^{2n-1}} \cdot \tau^{(2n)}(v_1)a^{2n}. \end{cases} \tag{11}$$

By analyzing the characteristics of Eqs. (9) and (11), we can obtain an important expression if we using the following superposition method.

$$\begin{aligned} Fun_k &= fun_1 - fun_3 + fun_5 + \ldots (-1)^{k-1} fun_{2k-1} = \sum_{n=1}^{k} (-1)^{n-1} fun_{2n-1} \\ &= \sin\psi_1 \cdot \left[\frac{H_0}{2} - H_2 + H_4 + \ldots (-1)^k H_{2k} + (-1)^{k-1}\frac{H_{2k}}{2} \right] \\ &= \sin\psi_1 \cdot \left[\tau\left(v_1\right) + (-1)^{k-1} \sum_{n=k}^{\infty} \frac{a^{n+k}}{(n+k)!} \frac{a^{n-k}}{(n-k)!} \frac{k}{n \cdot 2^{2n}} \tau^{(2n)}(v_1) \right] \\ &= \sin\psi_1 \cdot \Lambda_k, \quad k = 1,2\ldots. \end{aligned} \tag{12}$$

where Λ_k can be written as follows:

$$\begin{cases} \Lambda_1 = \tau\left(v_1\right) + \dfrac{\tau^{(2)}\left(v_1\right)a^2}{8} + \dfrac{\tau^{(4)}\left(v_1\right)a^4}{192} + \dfrac{\tau^{(6)}\left(v_1\right)a^6}{9216} + \ldots \\[2mm] \Lambda_2 = \tau\left(v_1\right) - \dfrac{\tau^{(4)}\left(v_1\right)a^4}{384} - \dfrac{\tau^{(6)}\left(v_1\right)a^6}{11520} + \ldots \\[2mm] \Lambda_3 = \tau\left(v_1\right) + \dfrac{\tau^{(6)}\left(v_1\right)a^6}{46080} + \ldots \\[2mm] \Lambda_k = \tau\left(v_1\right) + (-1)^{k-1} \displaystyle\sum_{n=k}^{\infty} \dfrac{a^{n+k}}{(n+k)!} \dfrac{a^{n-k}}{(n-k)!} \dfrac{k}{n \cdot 2^{2n}} \tau^{(2n)}(v_1). \end{cases} \tag{13}$$

As shown in Eq. (13), the second, the fourth, and the even higher-order terms (function of the modulation index, for an isolated transition, $m = a/\gamma$) cannot be eliminated in Λ_1 (the data of X and Y components of the first harmonic are used). Clearly, when the modulation depth is larger, contributions to Λ_1 made by the even higher-order terms, especially the second- and fourth-order terms become greater, which is consistent with the conclusion of G. Stewart's studies [8–12]. In our research, we found that the second-order term can be completely eliminated and the effects of the even higher-order terms (fourth, sixth, and so on) can be reduced when the first and third harmonics (Λ_2) are used. Similarly, the second- and fourth-order terms can be eliminated in Λ_3, and the second, fourth…up to $2(k$-1)-order terms can be eliminated in Λ_k, as shown in Eq. (13). Meanwhile, the sum of the even higher-order

terms $[2k, 2(k + 1)\ldots$order terms] in Λ_k can be near zero when k approaches infinity, as per the d'Alembert and Cauchy convergence principles, so we can obtain the following equation:

$$\Lambda_k\big|_{k\to\infty} = \tau(\nu_1) = \exp\big[-\alpha(\nu_1)\big]. \tag{14}$$

Taking into account Eq. (12), the following important equation can be obtained:

$$\exp\big[-\alpha(\nu_1)\big] = \tau(\nu_1) = \Lambda_k\big|_{k\to\infty} = \frac{Fun_k}{\sin\psi_1}\bigg|_{k\to\infty}. \tag{15}$$

The gas absorption shape can be recovered by the following expression:

$$\alpha(\nu_1) = -\ln\left(\frac{Fun_k}{\sin\psi_1}\right)\bigg|_{k\to\infty}, \tag{16}$$

where Fun_k are determined by data of the X and Y components of the odd harmonics in actual measurements, the phase shift ψ_1 between the intensity and frequency modulation can be determined by using the method described in literature [19].

3. Simulation results

In order to validate the reliability and precision of the method established in the current study, we took the NH_3/air mixture as the research object, and the transitions of NH_3 near 1531 nm are selected to recover the gas absorbance shape. The spectroscopic parameters of these transitions are shown in Table 1 [20].

Table 1. Spectroscopic Parameters for the Selected Transitions near 1531 nm (296K)

	ν_0 [cm^{-1}]	S [cm^{-2}/atm]	Lower state	Broadening [cm^{-1}/atm]		HWHM [cm^{-1}]		
			E'' [cm^{-1}]	γ_{self}	γ_{Air}	0.1atm	0.5atm	1.0atm
Line 1	6528.764	0.0594	277	0.598	0.0677	0.0150	0.0441	0.0848
Line 2	6528.894	0.0307	301	0.657	0.0758	0.0157	0.0487	0.0943
Line 3	6529.184	0.0322	266	0.535	0.0762	0.0154	0.0471	0.0911

The typical simulation results are shown in Fig. 1, where the black solid curve ($a = 0$) represents the calculation absorbance shape calculated by the spectroscopic parameters of the transitions, as shown in Table 1. Gas temperature, pressure, NH_3 concentration, absorption path length, and phase shift ψ_1 adopted in the simulation are 296 K, 0.1 atm, 3.0%, 25.5 cm, and 45.5°, respectively. Meanwhile, HWHM of each transition is listed in Table 1. Figure 1(a)~1(d) reflect the characteristics of the gas absorbance shape recovered by Λ_k ($k = 1, 2, 3, 4$), which are close to the calculation absorbance shape at decreasing modulation depth. In Fig. 1(a), the absorbance shape recovered by Λ_1 only agrees well with the calculation value when the modulation depth is less than 0.008 cm^{-1} ($m\approx0.5$), and the residual errors increase sharply with increasing modulation depth. Calculations show that the maximum error becomes higher than 25% when the modulation depth reaches 0.016 cm^{-1} ($m\approx1.0$). This phenomenon can be attributed to the even higher-order terms, especially the second- and fourth-order terms (as shown in Eq. (13), which have made significant contributions to Λ_1. The effects of these terms cannot be neglected at such a large modulation depth. Therefore, the method of G. Stewart et al.

cannot be used to recover the gas absorbance shape, especially the modulation index is larger than 0.2.

As noted in Eq. (13), the second-order term is completely eliminated and the effects of other even higher-order terms are reduced when Λ_2 is used. The simulation results show that the absorbance shape recovered by Λ_2 is in excellently agreement with the calculation value, even if the modulation depth reaches 0.016cm^{-1} ($m\approx1.0$), as shown in Fig. 1(b). Clearly, the results in Figs. 1(c) and 1(d) show that the modulation depths have a very small influence on the recovery of results when Λ_3 and Λ_4 are used. For example, the maximum residual errors are no more than 1.75%, even if the modulation depths reach 0.024 cm^{-1} ($m\approx1.5$) and 0.032 cm^{-1} ($m\approx2.0$), as shown in Figs. 1(c) and 1(d), respectively. In actual measurements, the modulation index is close to 2.0. Hence, the application of Λ_3 or Λ_4 to recover the gas absorbance shape is highly accurate in many cases. In addition, simulation results have shown that recovery accuracy can be further improved if the higher odd harmonics (ninth, eleventh, and so on) are used.
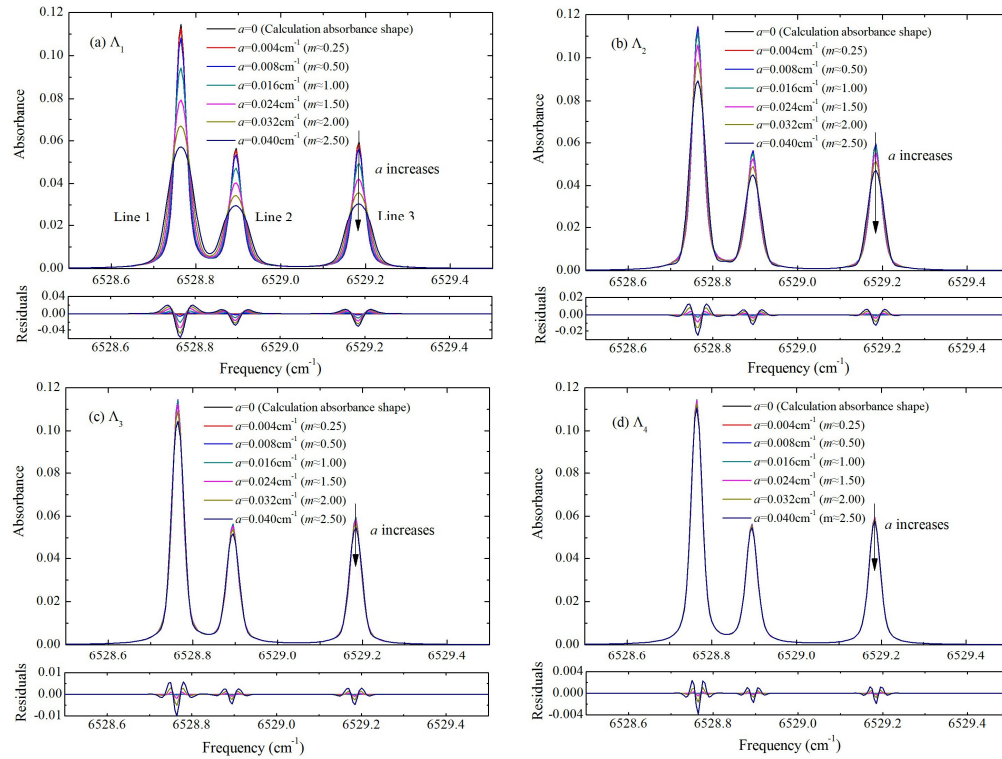

Fig. 1. Gas absorbance shape of NH_3 near 1531 nm recovered by Λ_k (k = 1, 2, 3, 4) at different modulation depths (P = 0.1atm, T = 296K, L = 25.5cm, X = 3.0%).

In Fig. 1, the three lines are independent of one another. To investigate the efficacy of this method in dealing with asymmetrical absorbance shape, we have used this method to recover the profile of these transitions when the pressure reaches the atmospheric level, and the three lines overlap one another. Figure 2 presents the typical simulation results, where gas temperature, pressure, NH_3 concentration, absorption path length, and phase shift ψ_1 adopted in the simulation are 296K, 1.0atm, 3.0%, 25.5cm, and 45.5°, respectively. HWHM of each transition is listed in Table 1. Similar to the characteristics in Fig. 1, Fig. 2 proves that the method established in the present paper can be used to recover a single transition and also can be applied under overlapping transitions.
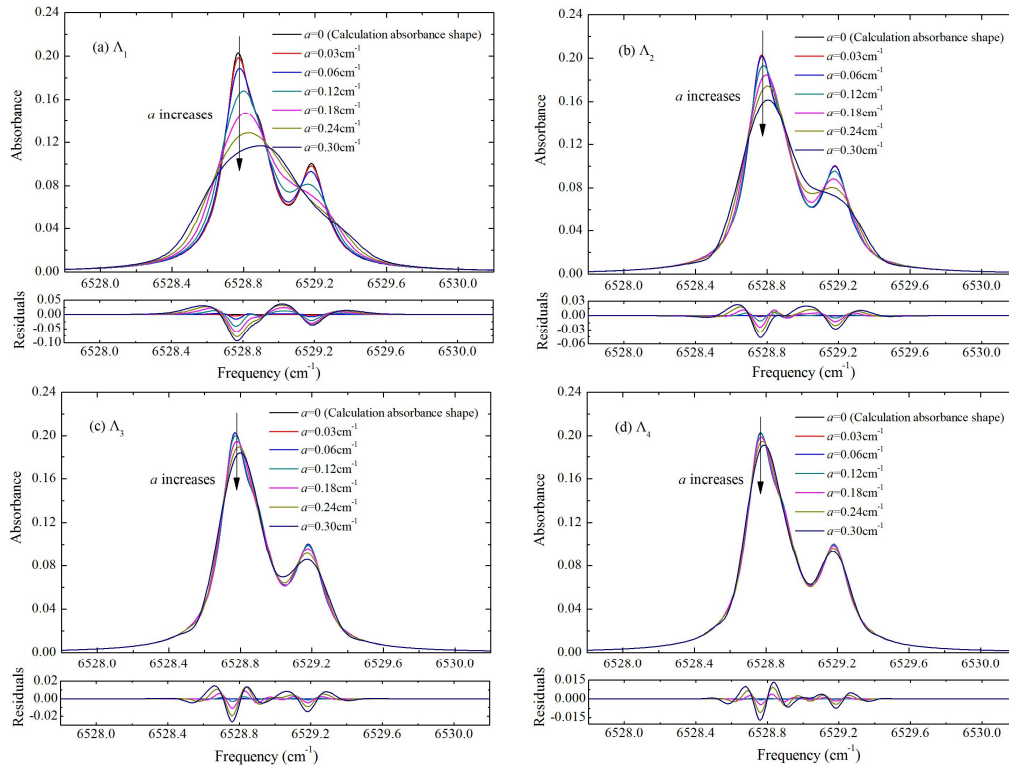
Fig. 2. Gas absorbance shape of NH$_3$ near 1531 nm recovered by Λ_k (k = 1,2,3,4) at different modulation depths (P = 1.0 atm, T = 296K, L = 25.5cm, X = 3.0%).

4. Experimental results

The diagram of the experimental setup is shown in Fig. 3. A fiber-coupled 1531.5 nm (6529 cm^{-1}) distributed feedback diode laser (NEL NLK1S5EAAA) manufactured by NTT Electronics Company is used as the spectroscopic source. The laser current and the temperature are controlled by a commercial diode laser controller (ITC4001). Light from the fiber-coupled diode laser is passed to a fiber collimator (Thorlabs F280FC-1550) and sent through the gas cell (25.5 cm length). The laser wavelength is measured using a free-space NIR wavelength meter (Bristol 621B). The optical power exiting from the cell is detected using a large surface Ge photodiode. An external modulation consisting of a 20 Hz sawtooth ramp with a faster 10 kHz sinusoidal modulation is fed into the diode laser controller. The phase shift ψ_1 between the intensity and frequency modulation can be determined using the method described in Ref [15]. In our experiments, the value is approximately 45.5° when the modulation frequency is 10 kHz. In addition, the modulation depth, scan range, and phase shift β between the reference and detection signals are adjusted to their optimum values according to the experimental requirements. The detector signals are recorded by a digital oscilloscope (DPO 4034B) and demodulated by a digital lock-in amplifier (SR830). Prior to each experiment, the gas cell is evacuated by a vacuum pump with an ultimate pressure of 1.0 Pa and filled with NH$_3$-Air mixture controlled by two mass flow controllers.
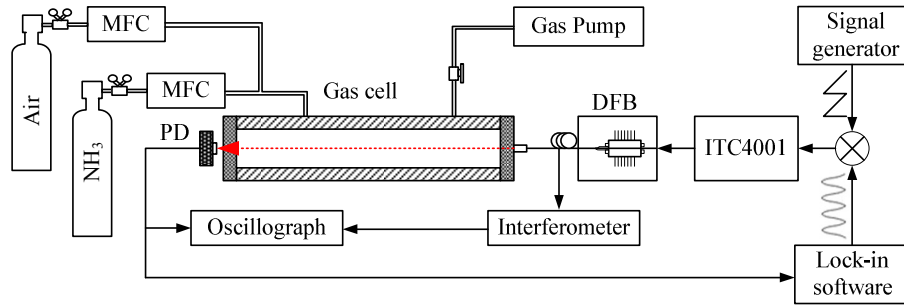
Fig. 3. Experimental set-up of the recovery of absorbance shape of NH_3 near 1531 nm.

As indicated Fig. 1, Line 3 is not interfered with by other lines (Lines 1 and 2) at low pressure (e.g., $P = 0.1$ atm). Hence, in the experiments, we can adjust the laser scanning range and allow it to scan only Line 3. Figure 4 shows a typical experiment result, where the phase shift ψ_1 is approximately 45.5° and the modulation depth is 0.03 cm^{-1}. In the experiment, gas temperature, pressure, NH_3 concentration, absorption path length, and phase shift β are 296 K, 0.1 atm, 3.0%, 25.5 cm and 135°, respectively. According to the experimental conditions, the modulation index can be calculated, and the obtained value is approximately 1.95. The data of X and Y components of the first, third, and fifth harmonics are shown in Fig. 4(a). The background of the first harmonic can be calculated using the data on both sides of X_1 and Y_1, where no NH_3 absorption exists ($X_{1\text{-}back} = 0$ mV, $Y_{1\text{-}back} = -100$ mV, and $S_{1\text{-}back} = 100$ mV). Subsequently, when the data of X and Y components of the first, third, and fifth harmonics are processed using our method, we can recover the absorbance shape, as shown in Fig. 4(b), where the black solid line represents the calculation absorption shape (6529.184 cm^{-1}), and the residual errors recovered by Λ_3 are shown in the bottom graph. In comparison with Fig. 1, the experiment results are in good agreement with the simulation results. The absorbance shapes recovered by Λ_1 and Λ_2 have become distorted because of the non-negligible effects of the second- and the fourth-order terms when the modulation index is approximately 1.95. However, the residual errors at the bottom figure graph show that the absorbance shape recovered by Λ_3 is close to the calculation value in the experiment.
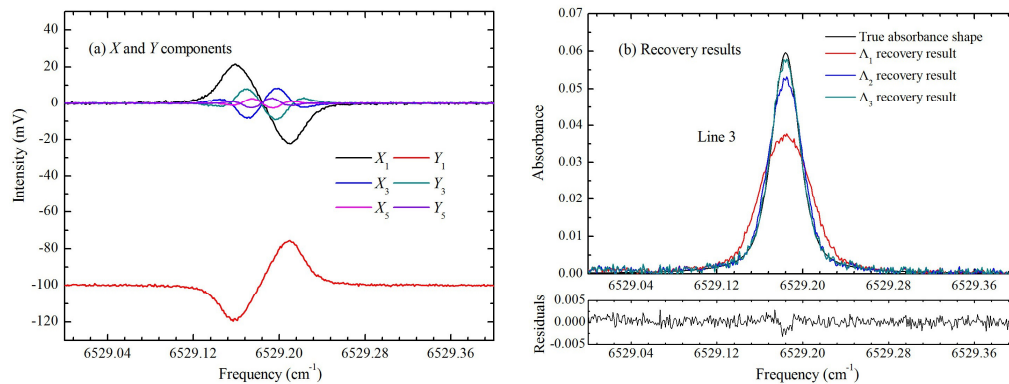

Fig. 4. (a) Experimental data of the X and Y components of the first, third and fifth harmonics; (b) absorbance shape recovered by Λ_k ($k = 1, 2, 3$) ($P = 0.1$atm, $T = 296$K, $L = 25.5$cm, $X = 3.0\%$, $m \approx 1.95$).

In the succeeding experiments, we fix the gas temperature, NH_3 concentration, absorption path length, and phase shift constants ($T = 296$K, $X = 3.0\%$, $L = 25.5$cm, $\psi_1 = 45.5°$), then use

Λ_4 to recover the absorbance shape under different pressure conditions (0.5 and 1.0 atm). As shown in Fig. 5, the absorbance shapes recovered by Λ_4 are close to the calculation values because the second, fourth, and sixth-order terms have been completely eliminated. Furthermore, if the higher odd harmonics (ninth, eleventh, and so on) are collected in actual measurements, recovery accuracy can be improved.
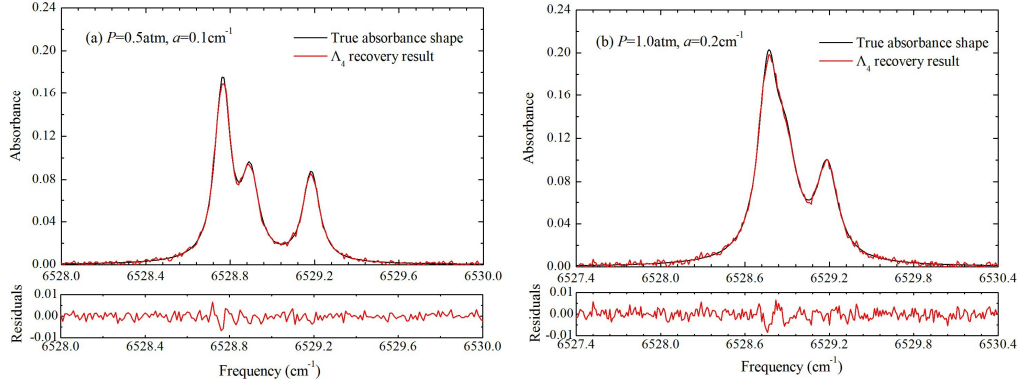

Fig. 5. Absorbance shape recovered by Λ_4 under different pressure conditions (T = 296 K, L = 25.5 cm, X = 3.0%, ψ_1 = 45.5°).

5. Conclusions

In the current paper, a method to recover gas absorbance shape with the odd harmonics of WMS is proposed. First, based on the absorption and harmonics theories, we have mathematically proven that the effects of the even higher-order terms can be completely eliminated when the data of the odd harmonics are processed using our method. Second, in order to validate the reliability and accuracy of this method, the transitions of NH_3 near 1531 nm are selected to recover the absorbance shapes using the numerical simulation and experimental techniques. Results of the simulation and the experiment show that the method established in this paper can work well for recovering gas absorbance shape in actual measurements, regardless of the value of the modulation index.

Acknowledgments